

# Polypeptide Nanocoatings for Preventing Dental and Orthopaedic Device-Associated Infection: pH-Induced Antibiotic Capture, Release, and Antibiotic Efficacy

Bingbing Jiang,<sup>1</sup> Bingyun Li<sup>1,2,3</sup>

<sup>1</sup> Biomaterials, Bioengineering & Nanotechnology Laboratory, Department of Orthopaedics, School of Medicine, West Virginia University, Morgantown, West Virginia

<sup>2</sup> WVNano Initiative, Morgantown, West Virginia

<sup>3</sup> Department of Chemical Engineering, College of Engineering and Mineral Resources, West Virginia University, Morgantown, West Virginia

Received 30 July 2007; revised 2 October 2007; accepted 9 October 2007

Published online 27 December 2007 in Wiley InterScience (www.interscience.wiley.com). DOI: 10.1002/jbm.b.31021

**Abstract:** Implant-associated infection is one of the most common and problematic complications for dental and orthopaedic patients. Modification of currently used implant surfaces aimed at bestowing them with antibacterial properties is a promising approach in the development of new biomaterials. In this study, a novel nanotechnology, that is, electrostatic self-assembly, was developed to construct biomimetic polypeptide nanocoatings on commonly used metal implants. A model antibacterial drug, cefazolin, was captured in the polypeptide nanocoating and its release was studied. We have shown that the capture and release of cefazolin was pH-induced and could be controlled, and the developed antibiotic-incorporated polypeptide multilayer nanocoatings could prevent *Staphylococcus aureus* colonization thus showing great potential for preventing implant-associated infection. © 2007 Wiley Periodicals, Inc. *J Biomed Mater Res Part B: Appl Biomater* 88B: 332–338, 2009

**Keywords:** bacterial adherence; surface modification; drug delivery/release; infection; nanotechnology

## INTRODUCTION

In dental and orthopaedic surgeries, bacterial contamination may cause serious complications. Removal of the infected implant is usually the only treatment option because the bacterial biofilm on the implant surface protects the microorganisms from the immune response and systemic antibiotic treatment. Consequently, implant-associated infection remains a primary barrier to the extended use of artificial implants,<sup>1–4</sup> and there is a substantial interest in developing implants with antibacterial properties.

It was estimated that 300,000 to 428,000 patients receive endosseous dental implants annually.<sup>5</sup> However, dental implant infection can occur and, like most medical implant-associated infection, this health problem stems from bacterial adhesion and biofilm formation on the implants. It is well known that bacterial adhesion and colonization to both implant and tissue surfaces are two impor-

tant steps in the pathogenesis of infection.<sup>6</sup> Clinical evaluations, review of retrieved implants, and *in vitro* studies have suggested that bacterial adhesion to an implant is an important step in the development of infection.<sup>7,8</sup>

To prevent infection, the commonly used strategy known as antibiotic therapy is aimed at killing bacteria.<sup>9</sup> A relatively new approach is to block bacterial adhesion that is the initial step of infection. Many strategies have been developed to inhibit bacterial adhesion, and increased interest has recently been focused on modifying the surface chemistry of implants to prevent bacterial adhesion.<sup>10</sup> The implant surface properties, for example hydrophilicity and surface charge, play a vital role in changing the interaction between bacteria and implant materials. For instance, increasing the surface hydrophilicity, thereby decreasing surface tension or surface energy, leads to reduced adhesion of a variety of bacteria. A negatively charged surface may lead to reduction of bacterial adhesion due to the increasing repulsion force between the implant surface and bacteria; the surfaces of most bacteria are negatively charged. Further, a surface coating with antibacterial properties has been shown to be very effective in preventing bacterial adhesion.<sup>11</sup>

Correspondence to: B. Li (e-mail: bli@hsc.wvu.edu)

Contract grant sponsors: WVU PSCoR, WVU Senate Grant, NASA WV EPSCoR

Many approaches of surface modification, such as dip coating, spin coating, and plasma spray, have been developed to achieve an antibacterial surface.<sup>12,13</sup> Among these techniques, electrostatic self-assembly is one of the most promising methods.<sup>14–17</sup> This self-assembly nanotechnology was mainly developed in the last two decades, and is based on alternative deposition of oppositely charged compounds, mainly polyelectrolytes, on a substrate.<sup>14</sup> Two significant characteristics of electrostatic self-assembly have made it attractive in potential medical applications: (i) a variety of materials can be used to control the surface properties, and (ii) the flexible choice of substrate geometry and surface configuration, and the simple process of coating may lead to potential commercial applications.

In this study, multilayer nanocoatings of synthetic polypeptides were constructed on commonly used metal implant surfaces using electrostatic self-assembly nanotechnology. Quartz slides were also used as substrates to monitor the self-assembly process by UV–vis spectroscopy. Polypeptides, that is poly(L-lysine) or PLL, and poly(L-glutamic acid) or PLGA, are biocompatible<sup>18</sup> and were used as coating materials. The outermost layer of the multilayer nanocoatings was PLGA, since PLGA is negatively charged and may help to prevent bacterial adhesion. pH-induced cefazolin capture and release in polypeptide nanocoatings was achieved as a novel local delivery system of antibiotics to inhibit bacterial adhesion thereby preventing potential infection. The developed pH-responsive nanocoating system may also be advantageous as a stimuli-responsive drug delivery system. The assembly process was monitored by UV–vis spectroscopy. Antibiotic capture and release from the multilayer polypeptide nanocoatings were studied at various pH values. Zone of inhibition tests were conducted to evaluate the antibacterial properties of the developed polypeptide nanocoatings against *Staphylococcus aureus* (*S. aureus*).

## MATERIALS AND METHODS

### Assembly of Polypeptide Multilayer Nanocoatings

Polypeptide multilayer nanocoatings were prepared on two types of substrates. Quartz slides were used to monitor the formation of polypeptide multilayer nanocoatings and the capture of cefazolin in the nanocoatings using UV–vis spectroscopy. Stainless steel discs were used as an implant model; stainless steel is one of the most commonly used implant materials in dental and orthopaedic applications. Stainless steel discs were used to prepare samples for Fourier transform infrared (FTIR) spectroscopy, drug-release, and antibacterial activity studies. Prior to use, the substrates, that is quartz slides and stainless steel discs, for preparing polypeptide multilayer nanocoatings were cleaned. The quartz slides, 25 mm × 10 mm × 1 mm, were cleaned by immersing them in piranha solution (3:1 H<sub>2</sub>SO<sub>4</sub>/H<sub>2</sub>O) for 2 h at 80°C, and rinsed with deionized

water. Stainless steel discs, 10 mm in diameter and 0.25 mm in thickness, were ultrasonicated in 70% ethanol/30% H<sub>2</sub>O for 0.5 h and rinsed with deionized water. Buffer solutions in the pH range 7.0–10.0 were prepared using Glycine-NaOH (50 mM) solutions. PLL (1 mg/mL) and PLGA (1 mg/mL) solutions were prepared by dissolving PLL and PLGA in the buffer solutions and mixing.

Polypeptide multilayer nanocoatings were prepared at pH 7.0 or 10.0. A precleaned quartz slide or stainless steel disc was immersed in PLL solution for 20 min, rinsed with buffer solution for 3 min, followed by air drying. The sample was then immersed in PLGA solution for 20 min, rinsed with buffer solution for 3 min, and air dried. Deposition of one layer of PLL and another layer of PLGA was referred to as one cycle. By repeating the deposition cycle, polypeptide multilayer nanocoatings with a desired number of bilayers, (PLL/PLGA)<sub>*n*</sub>, where *n* is the number of deposition cycles or bilayers, were obtained. The formation of polypeptide multilayer nanocoatings on quartz slides was monitored by UV–vis spectroscopy. The thickness of polypeptide multilayer nanocoatings was measured by ellipsometry.

### Capture of Antibiotic in Polypeptide Multilayer Nanocoatings

Antibiotics can be incorporated in polypeptide multilayer nanocoatings to prevent potential implant-associated infection. As an example, cefazolin was dissolved in three buffer solutions of pH 7.0, 8.0, and 9.0 at a concentration of 5 mg/mL. Quartz slides with polypeptide multilayer nanocoatings were immersed and incubated for 5 and 10 min in the antibiotic solutions at ambient temperature. After rinsing with deionized water, the samples were dried using N<sub>2</sub> gas. Capture of cefazolin in the polypeptide multilayer nanocoatings was confirmed by FTIR under reflection mode. The cefazolin capture efficiency for samples prepared at various pH values was determined by measuring their absorbance at 270 nm, a characteristic absorption peak of cefazolin, using UV–vis spectroscopy.

### In Vitro Antibiotic Release From Polypeptide Multilayer Nanocoatings

Stainless steel discs with polypeptide multilayer nanocoatings were immersed in 10 mL of phosphate buffer solution (PBS). A 0.6 mL sample of PBS was taken at a certain time period and analyzed by measuring its absorbance at 270 nm using UV–vis spectroscopy. Meanwhile, a 0.6 mL sample of fresh PBS of the same pH was added to keep a constant volume of the release medium. Raw data were converted to concentration (mg/mL) of cefazolin (*C<sub>n</sub>*) using the standard curve we obtained (data not shown). The total antibiotic release (*M<sub>n</sub>*) was calculated according to the following equation:

$$M_n = C_n \times V/A_n$$

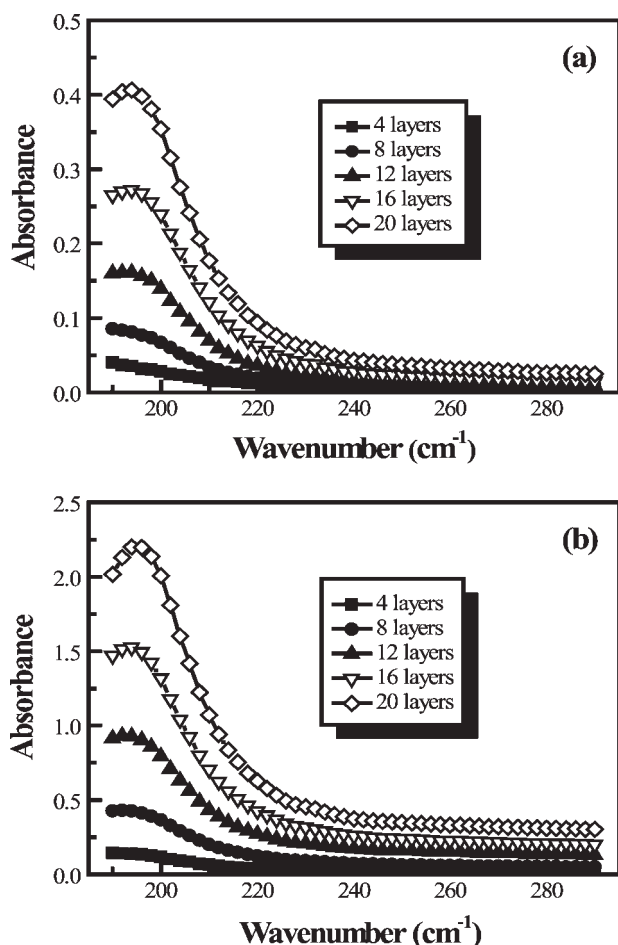


**Figure 1.** Preparation of PLL/PLGA multilayer nanocoatings on quartz slides at (a) pH 7.0 and (b) pH 10.0.

where  $V$  is the volume of the withdrawn medium,  $A_n$  is the surface area of coating on disc.

#### **In Vitro Antibacterial Activity Study**

Three types of samples were studied: stainless steel discs, stainless steel discs with polypeptide multilayer nanocoatings, and stainless steel discs with polypeptide multilayer nanocoatings with cefazolin. Polypeptide multilayer nanocoatings were prepared at pH 10.0. A modified Kirby-Bauer technique was used to assess the antibacterial activity of our developed polypeptide multilayer nanocoatings with antibiotics.<sup>19</sup> A clinical isolate of *S. aureus* was obtained and grown overnight in Trypticase soy broth to a suspension of  $10^8$  CFU/0.1 mL. A cotton swab was placed briefly in the *S. aureus* suspension and rubbed across the surface of a Trypticase soy agar plate. Then the three types of discs were inserted parallel to the plate surface, and the plates were incubated at 37°C for 24 h. The antibacterial activity was assessed by measuring the diameter of the zone of inhibition circling the discs. Six measurements were recorded for each sample, and the experiment was repeated thrice. The average diameters of the zones of inhibition were calculated.

## **RESULTS**

Polypeptide multilayer nanocoatings were prepared by electrostatic self-assembly nanotechnology. The formation of PLL/PLGA multilayer nanocoatings was examined by UV-vis and FTIR spectroscopy as well as scanning electron microscopy, SEM (Figures 1, 2, and 3). Figure 1 shows that the UV-vis absorbance of PLL/PLGA multilayer nanocoatings increased with an increasing number of deposition bilayers, and substantially higher UV-vis absorbance was observed for the samples prepared at pH 10.0 than at pH 7.0. The surface morphology of the samples with and without a polypeptide nanocoating was shown in Figure 2. The thickness of polypeptide multilayer nanocoatings was obtained by ellipsometry measurements. We found that the thickness per bilayer of samples prepared at pH 10.0 and 7.0 were  $12.0 \pm 0.3$  and  $6.6 \pm 0.5$  nm, respectively.

The formation of polypeptide multilayer nanocoatings on stainless steel discs was also demonstrated by FTIR spectroscopy. Intensity increasing in FTIR spectra was observed with an increasing number of bilayers (Figure 3). The capture of cefazolin was confirmed, as the appearance of a peak at  $1760\text{ cm}^{-1}$  corresponds to cefazolin lactam vibrate (C=O).

The influence of cefazolin solution pH on cefazolin loading was studied. Figure 4(a) represents the UV-vis absorbance of cefazolin contributing to the polypeptide multilayer nanocoatings on quartz slides. One can see that the absorbance increased with the decrease of pH, and more cefazolin was captured at pH 7.0 than at pH 8.0 and 9.0. Moreover, more cefazolin was captured at 10 min loading than at 5 min. Therefore, the capture of cefazolin can be tuned by the pH of the drug solution and also by the drug loading time.

The normal tissue has a pH of around 7.4 and the injured tissue has a pH 7.0, owing to disrupted blood



**Figure 2.** SEM images of stainless steel disc surfaces with and without (the inset) a polypeptide nanocoating. A scratch was made through the coating.

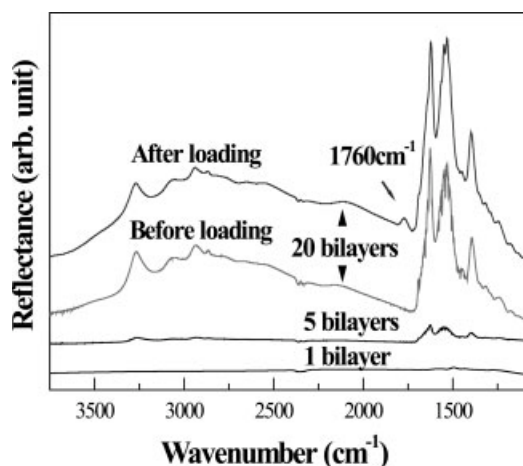


**Figure 3.** FTIR spectra of polypeptide multilayer nanocoatings on stainless steel discs. The absorbance peak at  $1760\text{ cm}^{-1}$  in the nanocoating after loading with cefazolin is due to lactam vibrate ( $\text{C}=\text{O}$ ) of cefazolin. The polypeptide multilayer nanocoatings were prepared at pH 10.0.

supply with concomitant waste accumulation (e.g.,  $\text{CO}_2$ ), and a change in tissue respiration to anaerobic, which produces lactic acid.<sup>20</sup> We studied the release of cefazolin from polypeptide multilayer nanocoatings in the pH range 7.0–10.0. We found that the pH of the releasing medium influenced the release profiles of cefazolin. Figure 4(b) shows that, in the pH range 7.0–10.0, cefazolin released more rapidly at a higher pH than at a lower pH, and more cefazolin was released at a higher pH. The amount of cefazolin released at pH 10.0 was twice that at pH 7.0, and a sustained cefazolin release up to 2 weeks was obtained.

Antibacterial activity of polypeptide multilayer nanocoatings incorporated with cefazolin was evaluated by a Kirby-Bauer technique. Figure 5 shows that stainless steel discs and stainless steel discs with polypeptide multilayer nanocoatings had no antibacterial effects, while stainless steel discs with polypeptide multilayer nanocoatings captured with cefazolin had antibacterial activity against *S. aureus*. The cefazolin-incorporated samples displayed a clear zone of inhibition with an average zone diameter of  $22.4 \pm 0.9$  mm.

## DISCUSSION

Bacteria are known to colonize metal implants and form adherent biofilms that retard the penetration of antibiotics to the underlying infection.<sup>3,21,22</sup> Prevention of postoperative infection remains a challenging problem in dental and orthopaedic surgeries. Modifying an implant with an antibacterial coating would inhibit bacteria from colonizing the implant surface and provide a high drug (e.g. antibiotic) concentration in a region commonly found as a nidus for infection. Such a coating system could prevent dental and orthopaedic implant-associated infection.

Our objectives were to establish the feasibility of developing polypeptide multilayer nanocoatings on dental and

orthopaedic implants using a recently developed nanotechnology and to incorporate antibiotics into the nanocoatings in a controlled means for potential infection prevention. We prepared polypeptide multilayer nanocoatings on stainless steel discs and quartz slides, and we introduced pH-induced capture and release of cefazolin to incorporate cefazolin in polypeptide multilayer nanocoatings.

Polypeptide multilayer nanocoatings were prepared using electrostatic self-assembly, which is mainly based on electrostatic attraction. Figure 6 shows a schematic diagram for the electrostatic self-assembly process, and the net charges of PLL and PLGA at various pH values, as well as the mechanism for our proposed pH-induced drug capture. Electrostatic self-assembly involves the repetitive sequential “dipping” of a substrate, for example a stainless steel disc or a quartz slide, in solutions of positively and negatively charged polyelectrolytes (i.e. PLL and PLGA). The polymers are deposited on the substrate and the surface

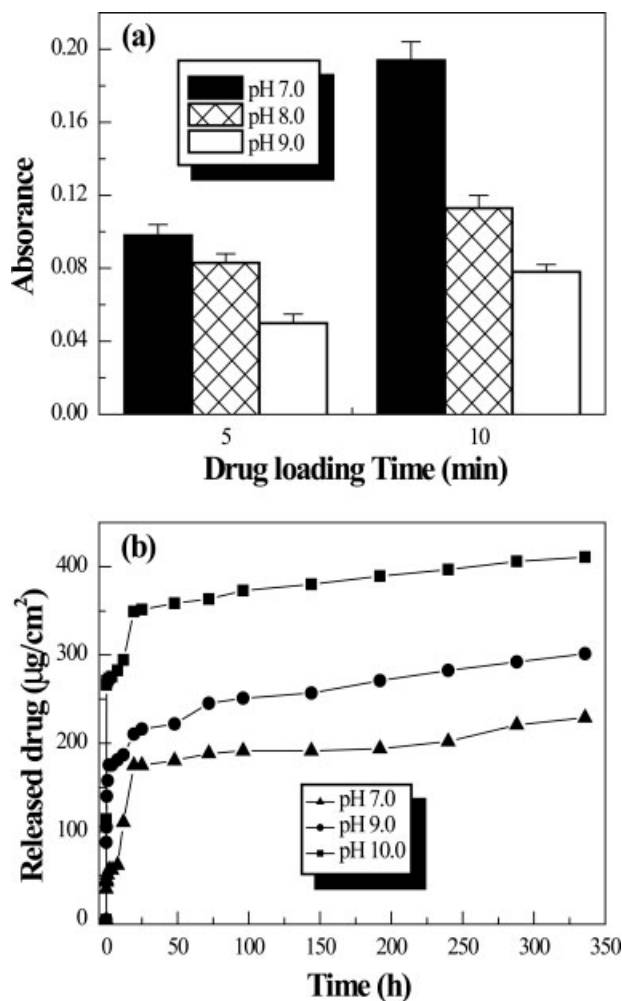


**Figure 4.** (a) Cefazolin loading in  $(\text{PLL/PLGA})_{40}$  multilayer nanocoatings at various pH values. The polypeptide multilayer nanocoatings were prepared at pH 10.0. (b) Release profiles of cefazolin from  $(\text{PLL/PLGA})_{40}$  coatings at various pH values (i.e. pH 7.0, 9.0, and 10.0). The polypeptide multilayer nanocoatings were prepared at pH 10.0, and cefazolin was captured at pH 7.0.

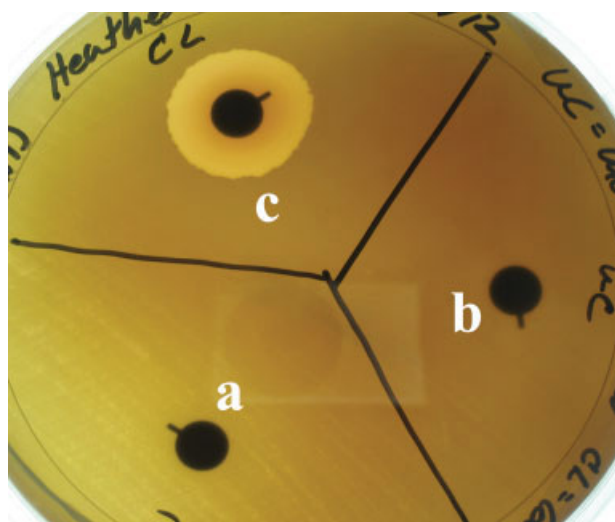


**Figure 5.** Zone of inhibition tests show that cefazolin incorporated in polypeptide multilayer nanocoatings can inhibit *S. aureus* growth. Three different types of stainless steel discs were used: (a) disc without coating, (b) disc coated with a polypeptide multilayer nanocoating, (c) disc coated with a polypeptide multilayer nanocoating and incorporated with cefazolin. [Color figure can be viewed in the online issue, which is available at [www.interscience.wiley.com](http://www.interscience.wiley.com).]

charge is reversed after each cycle. The method can yield a coating regardless of the surface area and shape of the support, and the properties of the coatings can be controlled on the nanometer scale.<sup>23,24</sup> By controlling the number, sequence, and type of polymer layers incorporated in the nanocoating, it is possible to create a wide variety of chemically and structurally diverse coatings.<sup>25</sup>

PLL and PLGA are water soluble and biodegradable.<sup>18</sup> Both PLL and PLGA are weak polyelectrolytes, and their net charges vary with pH (Figure 6): PLL is fully charged at a pH lower than 8.0 while its net charge decreases with increasing pH above 8.0. PLGA is fully charged at a pH above 6.0 while its net charge decreases with decreasing pH below 6.0. At pH 7.0, both PLL and PLGA are fully charged, while at pH 10.0, PLGA is fully charged and PLL becomes partially charged. As a result, more PLL molecules are needed at pH 10.0 than at pH 7.0 to match and overcharge the surface of its neighboring PLGA layer, and the charge repulsion among PLL molecules at pH 10.0 is smaller than at pH 7.0. These conditions led to higher absorbance and thicker bilayers of the polypeptide multilayer coatings prepared at pH 10.0 than at pH 7.0 (Figure 1).

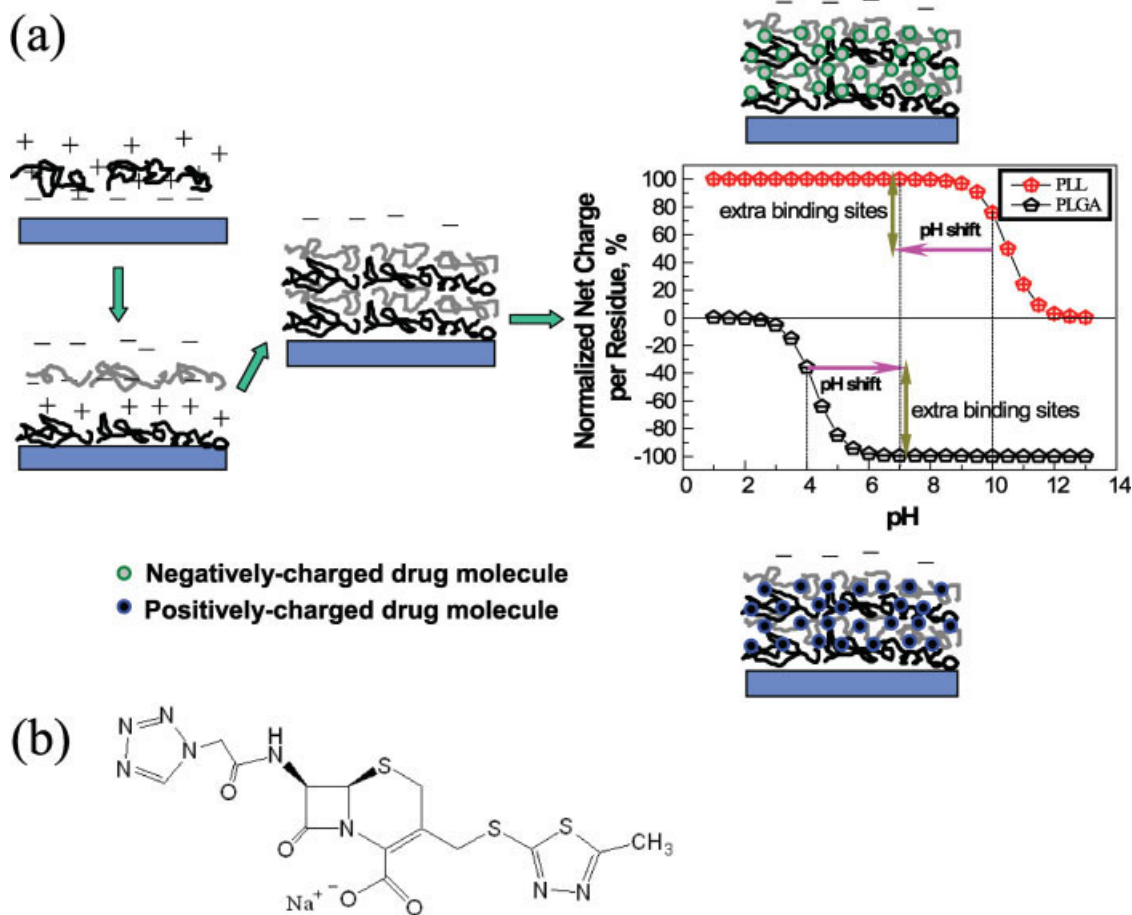


**Figure 6.** (a) Schematic diagram of polypeptide electrostatic self-assembly on a substrate, for example an implant model, and the net charges versus pH of PLL and PLGA, as well as the mechanism for drug loading. (b) Structure of cefazolin. [Color figure can be viewed in the online issue, which is available at [www.interscience.wiley.com](http://www.interscience.wiley.com).]

We incorporated cefazolin, an antibiotic, in polypeptide multilayer nanocoatings by pH-induced drug capture. As shown in Figure 6, if the (PLL/PLGA)<sub>n</sub> multilayer nanocoating is prepared at a higher pH, for example pH 10.0, the multilayer nanocoating allows you to incorporate negatively charged drug molecules [e.g. cefazolin, Figure 6(b)] at a lower pH, for example pH 7.0, 8.0, and 9.0, since PLL molecules in the nanocoatings provide extra positive charges upon the pH shifting from 10.0 to a lower pH. More cefazolin can be captured with decreasing pH from 9.0, to 8.0, and to 7.0 [Figure 4(a)], since more extra binding sites of PLL become available as pH decreases. Therefore, higher cefazolin capturing-capacity was achieved at lower pH [Figure 4(a)]. Similarly, positively charged drug molecules can be captured in (PLL/PLGA)<sub>n</sub> nanocoatings upon pH shifting to a higher pH, for example pH 7.0, if the nanocoatings are prepared at a lower pH, for example 4.0. pH-induced capture of cefazolin, negatively charged [Figure 6(b)], was confirmed by FTIR and UV-vis absorbance, as a lactam vibrate (C=O) peak of cefazolin at 1760 cm<sup>-1</sup> was observed (Figure 3), and the UV-vis absorbance at 270 nm increased with time after immersing the samples in cefazolin solutions [Figure 4(a)]. Different from most spin or other coatings, in the present study, the drug molecules were electrostatically bound to the coating component thereby their capture in the coating is more controllable and environmentally specific.

We studied the release profiles of cefazolin from polypeptide multilayer nanocoatings. The release of drug molecules from the polypeptide nanocoatings were due to the diffusion or loss of binding sites on PLL molecules if there was a pH shift from drug loading to drug release as shown in the present study. Figure 4(b) shows that cefazolin had a slower release rate at pH 7.0 than at pH 9.0 and 10.0, while in all cases there was a burst release. The higher incorporation [Figure 4(a)] and slower release [Figure 4(b)] at pH 7.0 were due to stronger binding of cefazolin to PLL molecules in the polypeptide multilayer nanocoatings at pH 7.0 than at higher pH values; the (PLL/PLGA)<sub>n</sub> nanocoatings were prepared at pH 10.0.

Incorporation of antibacterial drugs in implants was accomplished in the present study is a novel approach to endowing implant surfaces with antibacterial properties. We conducted zone of inhibition tests to evaluate the antibacterial effects of the developed cefazolin incorporated polypeptide multilayer nanocoatings. As shown in Figure 5, a highly significant reduction in bacterial growth was achieved in the antibiotic-incorporated stainless steel discs compared to the controls. The antibiotic-incorporated polypeptide multilayer nanocoatings can inhibit *S. aureus* colonization and have the potential to prevent infection.

Finally, it is worthwhile to point out that the use of local antibiotics offers the advantages of high local but low systemic antibiotic levels and potentially more thorough elimination of infection compared to systemic antibiotic therapy. The recently developed electrostatic self-assembly nano-

technology has the advantages, compared to other coating techniques, of fewer polymers to build the coating, more control over the structure of the nanocoating, and more control over the loading and release of drugs. Follow-up studies will be carried out, for instance, in an *in vivo* model we recently developed,<sup>26</sup> to investigate the efficacy of antibiotic-incorporated polypeptide multilayer nanocoatings in preventing infection *in vivo*.

## CONCLUSIONS

Polypeptide multilayer nanocoatings were prepared using a recently developed nanotechnology, that is electrostatic self-assembly. Cefazolin was incorporated into the nanocoatings, and the capture and release of cefazolin was pH-induced and can be controlled. We have shown that the antibiotic-incorporated polypeptide multilayer nanocoatings had antibacterial activity against *S. aureus*, and implants with such nanocoatings may be used prophylactically to reduce the incidence of implant-associated infection. This could offer the additional benefit of reducing implant colonization rates that necessitate costly implant removal or replacement. In addition, the developed approach may provide a novel stimuli-responsive local delivery system to prevent device-associated infection.

## REFERENCES

1. Bisno AL, Waldvogel FA, editors. Infections Associated With Indwelling Medical Devices. Washington, DC: American Society for Microbiology; 1989.
2. Sugarman B, Young EJ. Infections associated with prosthetic devices: Magnitude of the problem. *Infect Dis Clin North Am* 1989;3:1871-1898.
3. Chang CC, Merritt K. Infection at the site of implanted materials with and without preadhered bacteria. *J Orthop Res* 1994;12:526-531.
4. Schlegel U, Perren SM. Surgical of infection involving osteosynthesis implants: Implant design and resistance to local infection. *Injury* 2006;37:S67-S73.
5. Iacono VJ. Dental implants in periodontal therapy. *J Periodontol* 2000;71:1934-1942.
6. An Y, Friedman RJ, editors. Handbook of Bacterial Adhesion. Totowa, NJ: Humana Press; 2000.
7. Costerton JW, Cheng KJ, Geesey GG, Ladd TI, Nickel JC, Dasgupta M, Marrie TJ. Bacterial biofilms in nature and disease. *Annu Rev Microbiol* 1987;41:435-464.
8. Gristina AG, Oga M, Webb LX, Hobgood CD. Adherent bacterial colonization in the pathogenesis of osteomyelitis. *Science* 1985;228:990-993.
9. Kyriaki K, Evangelos JGB. Carrier systems for the local delivery of antibiotics in bone infections. *Drugs* 2000;59:1223-1232.
10. Jansen B. Current Approaches to Prevention of Catheter-Related Infection. New York, NY: Marcel Dekker; 1997.
11. Darouiche RO. Antimicrobial approaches for preventing infections associated with surgical implants. *Healthcare Epidemiol* 2003;36:1284-1289.
12. Li TT, Lee JH, Kobayashi T, Aoki H. Hydroxyapatite coating by dipping method, and bone bonding strength. *J Mater Sci Mater Med* 1996;7:355-357.

13. Muller-Buschbaum P, Gebhardt R, Maurer E, Bauer E, Gehrke R, Doster W. Thin casein films as prepared by spin-coating: Influence of film thickness and of pH. *Biomacromolecules* 2006;7:1773–1780.
14. Decher G. Fuzzy nanoassemblies: Toward layered polymeric multicomposites. *Science* 1997;277:1232–1237.
15. Cai KY, Rechtenbach A, Hao JY. Polysaccharide-protein surface modification of titanium via a layer-by-layer technique: Characterization and cell behavior aspects. *Biomaterials* 2005;26:5960–5971.
16. Scranton AB, Rangarajan B, Klier J. Biomedical applications of polyelectrolytes. *Adv Polym Sci* 1995;122:1–54.
17. Li B, Haynie DT. Multilayer biomimetics: Reversible covalent stabilization of a nanostructured biofilm. *Biomacromolecules* 2004;5:1667–1670.
18. Shih IL, Van YT, Shen MH. Biomedical applications of chemically and microbiologically synthesized poly(glutamic acid) and poly(lysine). *Mini Rev Med Chem* 2004;4:179–188.
19. Sherertz RJ, Forman DM, Solomon DD. Efficacy of dicloxacillin-coated polyurethane catheters in preventing subcutaneous *Staphylococcus aureus* infection in mice. *Antimicrob Agents Chemother* 1989;33:1174–1178.
20. Khamsi R. Smart drug kills pain and only the pain. *New Sci* 2007;194:11.
21. Gristina AG, Costerton JW. Bacterial adherence and the glycocalyx and their role in musculoskeletal infection. *Orthop Clin North Am* 1984;15:517–535.
22. Prewett AB, Domenick JM, Tsang N, O’Leary RK, Daniels AU. Differential adherence of three clinical isolates of staphylococcus to various metal surfaces. *Trans Soc Biomater* 1991;14:105–110.
23. Li B, Haynie DT, Palath N, Janisch D. Nanoscale biomimetics: Fabrication and optimization of stability of peptide-based thin films. *J Nanosci Nanotechnol* 2005;12:2042–2049.
24. Zhong Y, Li B, Haynie DT. Fine tuning of physical properties of designed polypeptide multilayer films by control of pH. *Biotechnol Prog* 2006;22:126–132.
25. Decher G, Schlenoff JB, editors. *Multilayer Thin Films: Sequential Assembly of Nanocomposite Materials*. Weinheim: Wiley-VCH; 2002.
26. Li B, Jiang B, Lindsey B, Boyce B, Salihu S, Kish V, Hubbard D. *In vitro* and *in vivo* studies of a novel system for cytokine local delivery. Annual Meeting of the Society for Biomaterials, Chicago, IL, April 2007.